

ORIGINAL ARTICLE

Oxidative stress induces mitochondrial dysfunction in a subset of autistic lymphoblastoid cell lines

S Rose, RE Frye, J Slattery, R Wynne, M Tippett, S Melnyk and SJ James

There is an increasing recognition that mitochondrial dysfunction is associated with autism spectrum disorders. However, little attention has been given to the etiology of mitochondrial dysfunction and how mitochondrial abnormalities might interact with other physiological disturbances such as oxidative stress. Reserve capacity is a measure of the ability of the mitochondria to respond to physiological stress. In this study, we demonstrate, for the first time, that lymphoblastoid cell lines (LCLs) derived from children with autistic disorder (AD) have an abnormal mitochondrial reserve capacity before and after exposure to reactive oxygen species (ROS). Ten (44%) of 22 AD LCLs exhibited abnormally high reserve capacity at baseline and a sharp depletion of reserve capacity when challenged with ROS. This depletion of reserve capacity was found to be directly related to an atypical simultaneous increase in both proton-leak respiration and adenosine triphosphate-linked respiration in response to increased ROS in this AD LCL subgroup. In this AD LCL subgroup, 48-hour pretreatment with *N*-acetylcysteine, a glutathione precursor, prevented these abnormalities and improved glutathione metabolism, suggesting a role for altered glutathione metabolism associated with this type of mitochondrial dysfunction. The results of this study suggest that a significant subgroup of AD children may have alterations in mitochondrial function, which could render them more vulnerable to a pro-oxidant microenvironment as well as intrinsic and extrinsic sources of ROS such as immune activation and pro-oxidant environmental toxins. These findings are consistent with the notion that AD is caused by a combination of genetic and environmental factors.

Translational Psychiatry (2014) 4, e377; doi:10.1038/tp.2014.15; published online 1 April 2014

INTRODUCTION

The autism spectrum disorders (ASDs) are a heterogeneous group of neurodevelopmental disorders defined by impairments in communication and social interaction along with restrictive and repetitive behaviors.¹ An estimated 1 out of 88 individuals in the United States are currently affected with an ASD and the incidence continues to rise.²

Mitochondrial dysfunction has become increasingly recognized as a major physiological disturbance in ASD.³ However, the etiology of mitochondrial dysfunction is not known. Indeed, although mitochondrial deoxyribonucleic acid mutations are commonly found in classical mitochondrial disease (MD), such mutations are only found in 23% of ASD children diagnosed with MD.³ This raises the possibility of acquired mitochondrial dysfunction as mitochondrial damage can result from environmental exposures implicated in ASD such as heavy metals,^{4–7} exhaust fumes,⁸ polychlorinated biphenyls⁹ or pesticides.^{10,11} Alternatively, mitochondria can be damaged by endogenous stressors associated with ASD such as elevated proinflammatory cytokines resulting from an activated immune system^{12–14} or other conditions associated with oxidative stress.^{15,16} The notion of an acquired mitochondrial disorder is supported by a recent twin study, which concluded that the environment contributes a greater percent of the risk of developing autistic disorder (AD, 55%) as compared with genetic factors (37%) with these factors contributing about equally for the broader ASD diagnosis.¹⁷

Oxidative stress may be a key link between mitochondrial dysfunction and ASD as reactive oxygen species (ROS) generated

from pro-oxidant environmental toxicants^{4–11} and activated immune cells^{3,18} can result in mitochondrial dysfunction.³ Four independent case-control studies have documented oxidative stress and oxidative damage in plasma, immune cells and post-mortem brain from ASD children.^{19–22} Interestingly, resting peripheral blood mononuclear cells and activated monocytes derived from children with ASD demonstrate a significant decrease in glutathione redox balance reflecting an intracellular deficit in glutathione-mediated antioxidant and detoxification capacity.²³

Lymphoblastoid cell lines (LCLs) are readily available in national and international biorepositories for many psychiatry and neurological diseases, including autism, and have been used as biological models for psychiatric and neurological disease, including the examination of genetic and metabolic aspects of these diseases. Developing a model of mitochondrial function for children with ASD using these cell lines would allow the detailed study of mitochondrial function as well as its associated metabolic abnormalities. We have previously demonstrated the cellular and mitochondrial redox imbalances in LCLs derived from children with AD.²⁰ Thus, in this study we hypothesized that LCLs derived from patients with AD are vulnerable to ROS, such that excessive intracellular ROS results in mitochondrial dysfunction. Furthermore, we hypothesize that this dysfunction only affects a subset of LCLs derived from children with AD. To this end, we examined mitochondrial respiratory activity in LCLs derived from AD children and unaffected control individuals. We demonstrate atypical changes in mitochondrial respiration in AD LCLs when exposed

to ROS in a subgroup of AD LCLs. We reveal the significance of glutathione metabolism in this effect by showing that pretreatment with *N*-acetylcysteine (NAC), a glutathione precursor, prevents mitochondrial vulnerability in the AD LCL subgroup that exhibit atypical responses to increased ROS.

MATERIALS AND METHODS

Lymphoblastoid cell lines and culture conditions

Twenty-two LCLs derived from white males diagnosed with AD chosen from pedigrees with at least one affected male sibling (mean/s.d. age 7.8 ± 3.1 year) were obtained from the Autism Genetic Resource Exchange (Los Angeles, CA, USA) or the National Institutes of Mental Health (Bethesda, MD, USA) center for collaborative genomic studies on mental disorders. Fourteen control LCLs derived from healthy white male donors with no documented behavioral or neurological disorder (mean/s.d. age 27.7 ± 9.1) were obtained from Coriell Cell Repository (Camden, NJ, USA) or the National Institutes of Mental Health. AD LCLs and control LCLs were randomly paired with each other (Supplementary Table S1). Young adult controls are standard in LCL studies due to low availability of younger ages.²⁰ On average, cells were studied at passage 12, with a maximum of 15. Genomic stability is very high at this low passage.^{24,25} Cells were maintained in RPMI 1640 culture medium with 15% FBS and 1% penicillin/streptomycin in a humidified incubator at 37 °C with 5% CO₂.

Seahorse assay

To measure mitochondrial function, we used the state-of-the-art Seahorse Extracellular Flux (XF) 96 Analyzer (Seahorse Bioscience, North Billerica, MA, USA). On the day of the assay, XF-PS plates were coated with 13 μ l poly-D-lysine (50 μ g ml⁻¹) for 2 h and washed twice with cell culture-grade water. One hour before the assay, cells were seeded onto coated 96-well XF-PS plates at a density of 1.1×10^5 cells/well in Dulbecco's modified Eagle's medium XF assay media (unbuffered Dulbecco's modified Eagle's medium supplemented with 11 mM glucose, 2 mM L-glutamax and 1 mM sodium pyruvate). Replicate/well varied from 4 to 8 depending on the number of cells available. Titrations determine the optimal concentrations of oligomycin (1.0 μ M), carbonyl cyanide-*p*-trifluoromethoxyphenyl-hydrizon (0.3 μ M), antimycin A (0.3 μ M) and rotenone (1.0 μ M). By sequentially adding these pharmacological agents to the respiring cells, we measured the basal respiration, adenosine-5'-triphosphate-linked respiration, PLR and RC (see Figure 1).

Redox challenge

ROS was increased *in vitro* by exposing cells to increasing concentrations of the redox cycling agent DMNQ for 1 h before the Seahorse assay. DMNQ enters cells and generates both superoxide and hydrogen peroxide similar to that generated by NADPH oxidase *in vivo*.²⁶ A 5 mg ml⁻¹ DMNQ solution was diluted in Dulbecco's modified Eagle's medium XF assay media into 10X stocks and added to cells in an XF-PS plate and incubated for 1 h at 37 °C in a non-CO₂ incubator. The concentrations of DMNQ were optimized as 5, 10, 12.5 and 15 μ M.

NAC rescue

To determine whether pretreatment with a glutathione precursor could rescue atypical responses to the ROS challenge, AD LCLs were plated in T25 flasks at a density of 5×10^5 cells ml⁻¹ in culture media with or without 1 mM NAC for 48 h. Cells were washed twice in Dulbecco's modified Eagle's medium XF media to remove any remaining NAC before DMNQ treatment and Seahorse assays. The control LCLs were not treated with NAC as they demonstrate normal glutathione metabolism.

Glutathione measurements

Approximately 2×10^6 viable cells were pelleted and snap-frozen on dry ice. Samples were stored at -80 °C until HPLC quantification of intracellular free GSH and GSSG.²⁷ Thawed cells were lysed by 3 s sonication in 112.5 μ l ice-cold phosphate-buffered saline followed by the addition of 37.5 μ l ice-cold 10% meta-phosphoric acid. This mixture was incubated for 30 min on ice followed by centrifuging for 15 min at 18 000 \times g at 4 °C. Results are expressed as nmol mg⁻¹ protein using BCA Protein Assay Kit (Pierce, Rockford, IL, USA).

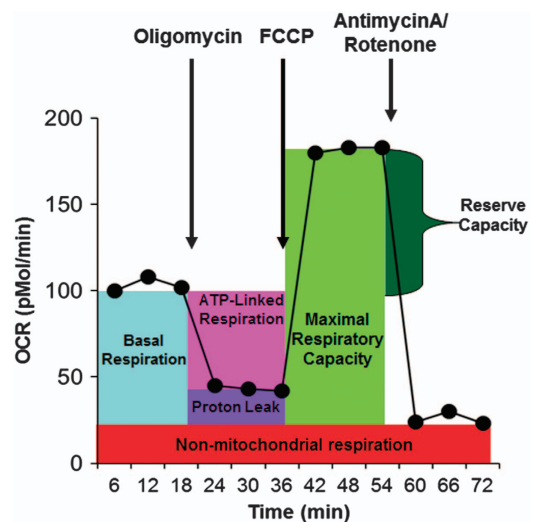


Figure 1. The Seahorse assay. Oxygen consumption rate is measured before and after adding pharmacological agents to respiring cells. Measurement of oxygen consumption over 6 min is made repeatedly. Three measurements are made and averaged to provide reliable measurements. For the first 18 min, total cellular oxygen consumption is measured. Basal respiration can be calculated from this quantity by subtracting non-mitochondrial respiration. Next oligomycin, an inhibitor of adenosine-5'-triphosphate (ATP) respiration, is added and a measurement of this is made over the next 18 min. This quantity can be subtracted from the total cellular oxygen consumption to determine ATP-linked respiration and non-mitochondrial respiration can be subtracted from this quantity to obtain proton-leak respiration. Next carbonyl cyanide-*p*-trifluoromethoxyphenyl-hydrizon, a protonophore, is added and a measurement of this is made over the next 18 min. The protonophore collapses the inner membrane gradient by making the inner membrane permeable to protons. This drives the electron transport chain to function at its maximum rate. Subtracting non-mitochondrial respiration from this quantity produces a measure of maximum respiratory capacity. Finally antimycin A, a complex III inhibitor, and rotenone, a complex I inhibitor, are added to shut down electron transport chain function. The resulting measurement over the next 18 min represents non-mitochondrial respiration, a measurement that can be used with the other measurements to calculate respiratory parameters. Finally, reserve capacity is calculated by subtracting basal respiration from maximum respiratory capacity.

Analytic approach

A mixed-effects regression²⁸ was conducted via SAS version 9.3 (Cary, NC, USA) 'glmmix' procedure. The mixed-effects models allowed data from each AD LCL to be compared with the paired control LCL run on the same plate. The mitochondrial respiratory measurement was the response variable with a between-group dichotomous effect (AD vs control, AD +NAC vs control) and within-group repeated factors of DMNQ concentration (modeled as a multilevel factor) as well as the interaction between these effects. We present the overall difference between the two comparison groups (group effect), the overall effect of the DMNQ concentration (DMNQ effect), and whether the effect of DMNQ concentration was different between the two groups (DMNQ \times group interaction). Random effects included the intercept and DMNQ. F-tests were used to evaluate significance. Planned *post hoc* orthogonal contrasts were used when the interaction was significant.

Differences in glutathione measurements between control and AD LCLs without DMNQ exposure were analyzed using a similar mixed-effect regression model. A general linear model was used to verify the DMNQ effect on AD and control LCLs as these LCLs were not matched. DMNQ was treated as a continuous variable since a dose response effect was expected.

Cluster analysis was conducted using Ward's technique.²⁹ Ward's technique defines the distance between clusters in terms of the between cluster variability to the within cluster variability. By examining the

dendrogram and several statistics (pseudo-F and *t*), a judgment is made about the number of clusters.³⁰

RESULTS

Verification of 2,3-dimethoxy-1,4-naphthoquinone (DMNQ) effect on LCL glutathione redox state

Glutathione concentrations were measured in three control and five AD LCLs at 2,3-dimethoxy-1,4-naphthoquinone (DMNQ) concentrations of 0, 1, 5, 10, 12.5 and 15 μM . DMNQ significantly decreased reduced glutathione (GSH) ($F(1,35)=52.45$, $P<0.001$) and GSH/oxidized glutathione (GSSG) ($F(1,35)=30.21$, $P<0.001$) and increased GSSG ($F(1,35)=13.80$, $P<0.001$) in a linear fashion (see Supplementary Figure S1). These changes were not different across groups.

Mitochondrial function in AD LCLs with ROS challenge

Basal respiration was greater overall in AD LCLs ($F(1,105)=10.02$, $P<0.005$) and significantly increased as DMNQ increased ($F(4,84)=6.22$, $P<0.0005$) (Figure 2a). This increase was significantly greater in AD LCLs ($F(4,105)=5.20$, $P<0.001$), due to a significantly higher basal respiration in AD LCLs at 10 μM ($t(105)=4.42$, $P<0.0001$) and 12.5 μM ($t(105)=3.21$, $P<0.005$). Basal respiration is composed of proton-leak respiration (PLR) and Adenosine-5'-triphosphate-Linked Respiration (ALR), which we examined separately.

Overall ALR was higher for AD LCLs ($F(1,105)=5.84$, $P<0.05$) (Figure 2b). ALR increased as DMNQ was increased ($F(4,84)=5.44$, $P<0.001$) with this increase significantly greater in AD LCLs ($F(4,105)=3.97$, $P<0.005$), due to significantly higher ALR in AD LCLs at 10 μM ($t(105)=3.86$, $P<0.0005$) with borderline significance at 12.5 μM ($t(105)=1.78$, $P<0.10$).

PLR was overall greater in AD LCLs ($F(1,105)=21.05$, $P<0.0001$) (Figure 2c) and significantly increased as DMNQ increased ($F(4,84)=11.31$, $P<0.0001$). This increase was significantly greater for AD LCLs ($F(4,105)=4.29$, $P=0.005$), due to a significantly higher PLR in AD LCLs at 10 μM ($t(105)=3.75$, $P<0.0005$) and 12.5 μM ($t(105)=4.71$, $P<0.0001$) (Figure 2c).

Maximal respiratory capacity (MRC) was overall significantly higher in AD LCLs ($F(1,105)=6.76$, $P=0.01$). Both LCL groups showed a significant (and similar) decrease in MRC as DMNQ increased ($F(4,84)=35.88$, $P<0.0001$) (Figure 2d).

As DMNQ increased, reserve capacity (RC) decreased ($F(4,84)=50.52$, $P<0.0001$) with this decrease significantly greater for AD LCLs ($F(4,105)=6.16$, $P<0.0005$). RC of AD LCLs was significantly higher than control LCLs without DMNQ ($t(105)=2.86$, $P=0.005$) and at 5 μM ($t(105)=2.73$, $P<0.01$) but then sharply dropped to be significantly lower than control LCLs at 10 μM DMNQ ($t(105)=2.44$, $P<0.05$) (Figure 2e).

Defining subgroups of AD LCLs

As AD and control LCLs differed markedly in the changes in ALR and PLR with DMNQ challenge, we examined whether the changes in these respiratory parameters could differentiate AD LCL subgroups. As the increase in ALR and PLR peaked at 10 μM DMNQ, the slope of the change in ALR and PLR from 0 to 10 μM DMNQ was calculated and entered into a cluster analysis. The cluster analysis divided the LCLs into two groups: AD-N ($n=12$) and AD-A ($n=10$) (pseudo-F 17.1, pseudo *t*-squared 18.3) (see Figure 3). The dendrogram (not shown) demonstrated clear differences between these groups.

The most striking difference between the two groups was the relationship between the change in PLR and ALR. For the AD-N group, there was a significant negative relationship between PLR and ALR (Figure 3a, $r=-0.77$, $P<0.01$, green line) such that an increase in PLR was associated with a decrease in ALR (and vice versa). If the two AD-N outliers were removed, the correlation remained high for AD-N LCLs ($r=-0.86$, $P<0.01$; blue line). Overall, there was little change in PLR and ALR with the DMNQ challenge in the AD-N subgroup (Figures 3b and c, green dashed lines).

For the AD-A subgroup, the relationship between PLR and ALR was different than the AD-N subgroup. Specifically, PLR and ALR both increased together (Figure 4a, $r=0.44$, $P=NS$, red line; Figures 3d and e, red dashed lines), rather than having an inverse relationship.

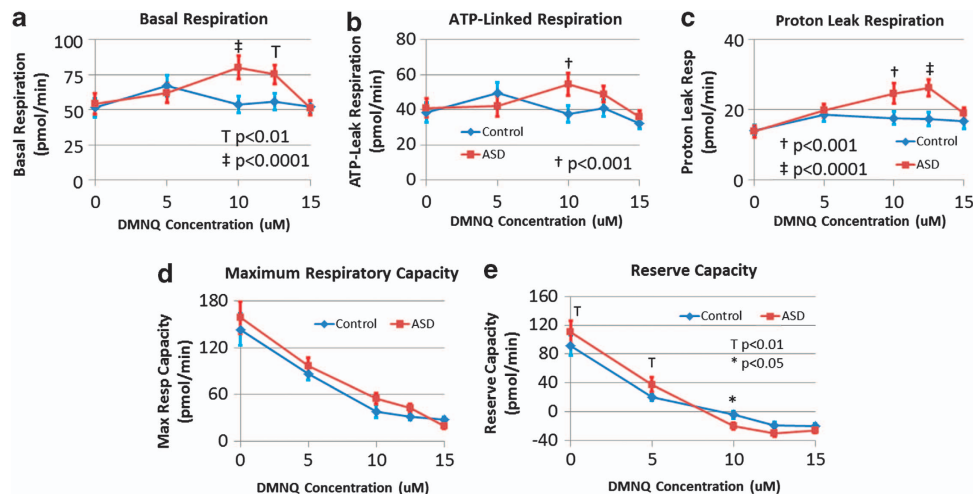


Figure 2. Lymphoblastoid cell lines (LCLs) derived from children with autistic disorder (AD) demonstrate differences in mitochondrial function as compared with control LCLs at baseline and after exposure to the redox cycling agent 2,3-dimethoxy-1,4-naphthoquinone (DMNQ) at four concentrations (5, 10, 12.5 and 15 μM) one hour before the assay. (a) Basal respiration increases as DMNQ concentration increases in the AD LCLs and becomes significantly higher in the AD LCLs at 10 and 12.5 μM DMNQ; (b) adenosine-5'-triphosphate-linked respiration increases as DMNQ concentration increases in the AD LCLs and becomes significantly higher in the AD LCLs at 10 μM DMNQ; (c) proton-leak respiration increases as DMNQ concentration increases in the AD LCLs and becomes significantly higher in the AD LCLs at 10 and 12.5 μM DMNQ; (d) maximum respiratory capacity decreased as DMNQ increased for both AD and control LCLs but overall AD LCLs demonstrated a higher maximum respiratory capacity; (e) reserve capacity decreases as DMNQ increases for both AD and control LCLs but the decline in reserve capacity is much sharper for the AD LCLs as compared with the control LCLs due to the fact that reserve capacity is significantly higher in the AD LCLs at low DMNQ concentrations but becomes significantly lower in the AD LCL at higher DMNQ concentrations.

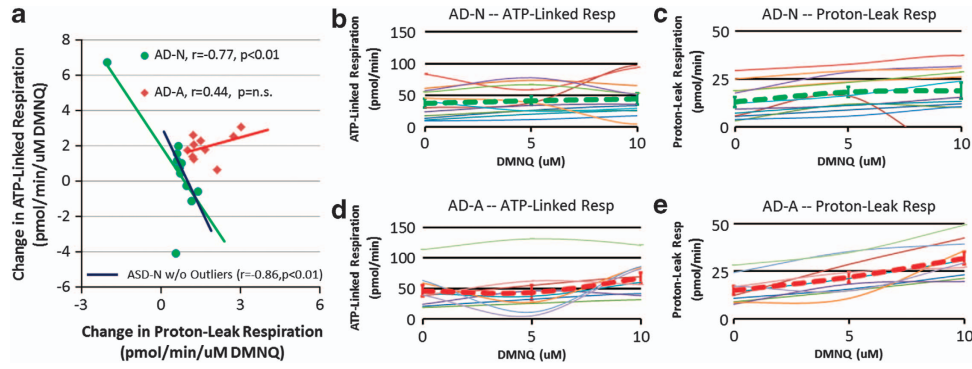


Figure 3. Clustering of lymphoblastoid cell lines (LCLs) derived from children with autistic disorder (AD) into two subgroups: the AD-N subgroup has mitochondrial respiratory profiles similar to controls and the AD-A subgroup has atypical mitochondrial respiratory profiles. (a) AD-N cases (green circles) and AD-A cases (red diamonds) represent the two subgroups. The AD-N subgroup demonstrates a negative correlation between adenosine-5'-triphosphate (ATP)-linked respiration and proton-leak respiration ($r = -0.77$, $P < 0.01$, green line) whereas the AD-A group demonstrates a positive correlation between ATP-linked respiration and proton-leak respiration ($r = 0.44$, $P = \text{NS}$, red line). If the two outliers are removed from the AD-N group, the correlation is still significant ($r = -0.86$, $P < 0.01$; blue line). (b) Individual (thin lines) and overall (thick green dashed line) change in ATP-linked respiration for the AD-N groups. Notice that there is little change overall. (c) Individual (thin lines) and overall (thick green dashed line) change in proton-leak respiration for the AD-N groups. Notice that there is little change overall. (d) Individual (thin lines) and overall (thick red dashed line) change in ATP-linked respiration for the AD-A groups. Notice that, overall, ATP-linked respiration increases with DMNQ concentration. (e) Individual (thin lines) and overall (thick red dashed line) change in proton-leak respiration for the AD-A groups. Notice that, overall, proton-leak respiration increases with DMNQ concentration. DMNQ, 2,3-dimethoxy-1,4-naphthoquinone; NS, not significant.

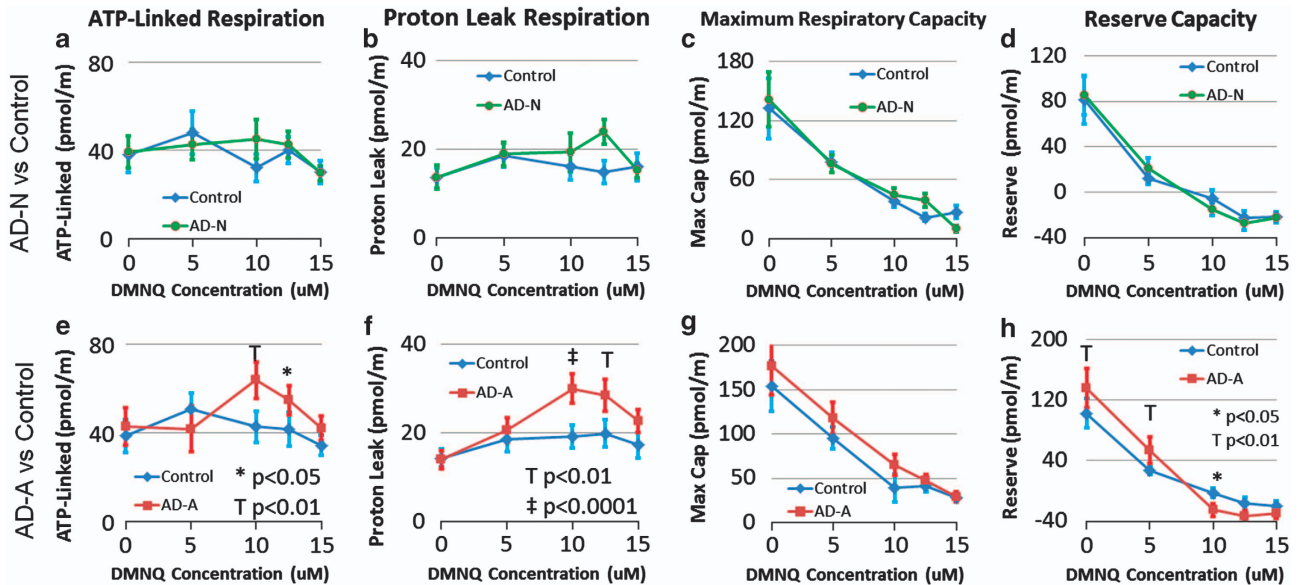


Figure 4. Seahorse respiratory measurements in two subgroups of lymphoblastoid cell lines (LCLs) derived from children with autistic disorder (AD) as compared with control LCLs at baseline and after exposure to the redox cycling agent 2,3-dimethoxy-1,4-naphthoquinone (DMNQ) at four concentrations (5, 10, 12.5 and 15 μM) one hour before the assay. Overall, the AD-A subgroup (e–h) parallels the differences between the AD and control LCLs found in the overall analysis whereas the AD-N subgroup (a–d) demonstrates similar mitochondrial response between the AD LCLs and control LCLs. For the AD-N subgroup (a) adenosine-5'-triphosphate(ATP)-linked respiration, (b) proton-leak respiration, (c) maximum respiratory capacity and (d) reserve capacity are similar between the AD and control LCLs. For the AD-A subgroup, (e) ATP-linked respiration increases as DMNQ concentration increases in the AD-A LCLs and becomes significantly higher in the AD-A LCLs at 10 μM DMNQ; (f) proton-leak respiration increases as DMNQ concentration increases in the AD-A LCLs and becomes significantly higher in the AD-A LCLs at 10 μM and 12.5 μM DMNQ; (g) maximum respiratory capacity decreased as DMNQ increased for both AD-A and control LCLs but overall AD-A LCLs demonstrated a higher maximum respiratory capacity; (h) the decline in reserve capacity is much sharper for the AD-A LCLs as compared with the control LCLs due to the fact that reserve capacity is significantly higher in the AD-A LCLs at low DMNQ concentrations but becomes significantly lower in the AD-A LCL at higher DMNQ concentrations.

As a comparison, the relationship between the PLR and ALR was examined for the control LCLs. The relationship between PLR and ALR for the control LCLs was found to be significantly positive ($r = 0.79$, $P < 0.01$; not shown).

Mitochondrial function in AD LCLs subgroups with ROS challenge
To better understand the differences between the AD LCL subgroups, we compared the AD LCLs with their paired control LCLs within each subgroup. Basal respiration is not shown as it is the combination of ALR and PLR.

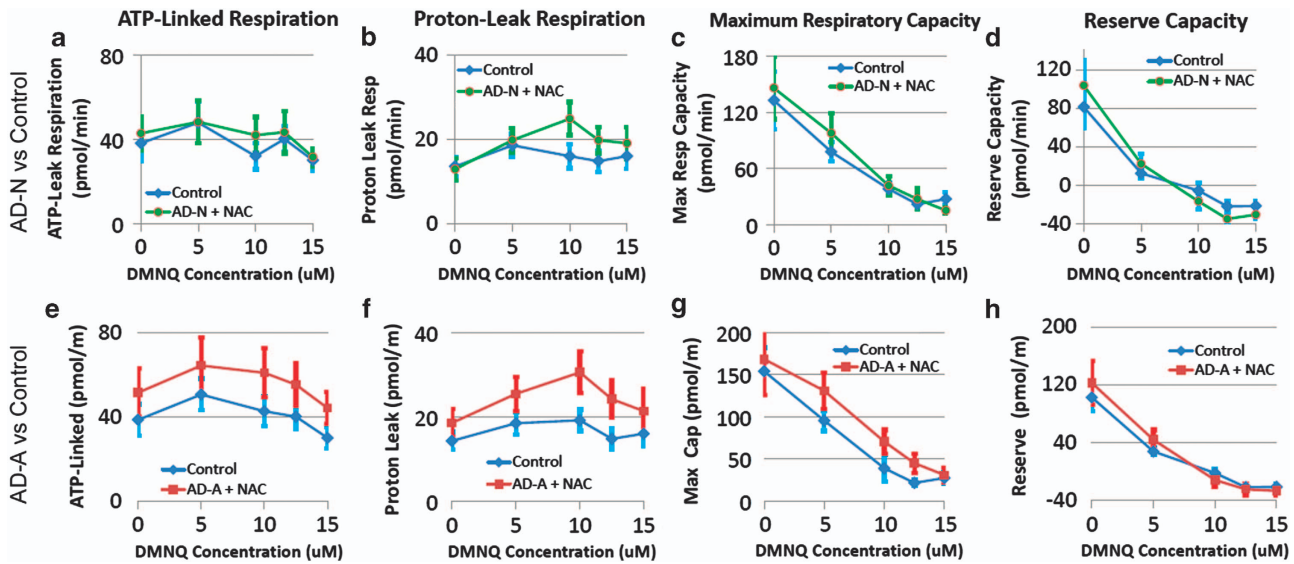


Figure 5. Seahorse respiratory measurements in two subgroups of lymphoblastoid cell lines (LCLs) derived from children with autistic disorder (AD) after 48 h incubation with 1 mM of *N*-acetyl-cysteine (NAC) as compared with control LCLs at baseline and after exposure to the redox cycling agent 2,3-dimethoxy-1,4-naphthoquinone (DMNQ) at four concentrations (5, 10, 12.5 and 15 μ M) one hour before the assay. Overall, atypical changes in mitochondrial function with increased DMNQ seen in the AD-A subgroup (**e–h**) are rescued with NAC treatment whereas NAC does not alter the dynamics of mitochondrial function in the AD-N subgroup (**a–d**). For the AD-N subgroup (**a**) adenosine-5'-triphosphate (atp)-linked respiration, (**b**) proton-leak respiration, (**c**) maximum respiratory capacity and (**d**) reserve capacity are similar between the AD and control LCLs. For the AD-A subgroup, changes (**e**) ATP-linked respiration, (**f**) proton-leak respiration, (**g**) maximum respiratory capacity and (**h**) reserve capacity with increasing DMNQ did not differ between the AD-A and control LCLs. However, (**e**) ATP-linked respiration, (**f**) proton-leak respiration and (**g**) maximum respiratory capacity were found to be overall greater in the AD-A LCLs as compared with control LCLs. This change in the overall function of the AD-A LCLs with NAC pretreatment normalized the reserve capacity differences between the AD-A and control LCLs.

AD-N LCLs. ALR, PLR, MRC and RC significantly changed as DMNQ increased in both AD-N and control LCLs ($F(4,40) = 3.22, P < 0.05$; $F(4,40) = 3.13, P < 0.05$; $F(4,40) = 15.92, P < 0.0001$; $F(4,40) = 22.74, P < 0.0001$, respectively) (Figures 4a–d), but this change was not significantly different between the LCL groups. The AD-N LCLs did not demonstrate any overall differences from controls for any of these respiration parameters.

AD-A LCLs. Overall, ALR was higher for AD-A LCLs ($F(1,50) = 6.46, P = 0.01$) (Figure 4e). ALR significantly increased as DMNQ increased in both LCL groups ($F(4,40) = 3.37, P < 0.05$) with this increase significantly greater for AD-A LCLs ($F(4,50) = 2.92, P < 0.05$), due to a greater ALR in the AD-A LCLs at 10 μ M ($t(50) = 3.23, P < 0.01$) and 12.5 μ M ($t(50) = 2.02, P < 0.05$).

PLR was overall higher for the AD-A LCLs ($F(1,50) = 24.31, P < 0.0001$) (Figure 4f). Increasing DMNQ resulted in a significant increase in PLR ($F(4,40) = 12.52, P < 0.0001$) with this increase significantly greater for the AD-A LCLs ($F(4,50) = 3.60, P = 0.01$), due to PLR being significantly higher in the AD-A LCLs at 10 μ M ($t(50) = 4.48, P < 0.0001$) and 12.5 μ M ($t(50) = 3.56, P < 0.001$).

MR decreased as DMNQ increased ($F(4,40) = 19.63, P < 0.0001$) and was overall significantly greater for the AD-A LCLs ($F(1,50) = 9.58, P < 0.005$) (Figure 4g).

RC decreased as DMNQ increased ($F(4,40) = 28.41, P < 0.0001$) with this decrease significantly more marked for AD-A LCLs ($F(4,50) = 6.08, P = 0.0005$) (Figure 4h). This was due to the RC being significantly higher in AD-A LCLs at low DMNQ concentrations (0 μ M $t(50) = 3.18, P < 0.005$; 5 μ M $t(50) = 2.56, P = 0.01$) and then plummeting so that RC was significantly lower in the AD-A LCLs at 10 μ M (10 μ M $t(50) = 2.16, P < 0.05$).

N-acetyl-L-cysteine rescues AD LCL RC abnormalities

AD LCLs were pre-treated with NAC to determine whether improving glutathione metabolism could normalize mitochondrial function.

AD-N NAC-treated LCLs. ALR, PLR, MRC and RC significantly changed as DMNQ increased ($F(4,40) = 3.04, P < 0.05$; $F(4,40) = 3.13, P < 0.05$; $F(4,40) = 15.92, P < 0.0001$; $F(4,40) = 22.74, P < 0.0001$, respectively) (Figures 5a–d), but this change was not significantly different between the LCL groups. The AD-N LCLs did not demonstrate any overall differences from their matched controls for any respiration parameter.

AD-A NAC-treated LCLs. ALR, PLR, MRC and RC significantly changed as DMNQ increased ($F(4,40) = 4.09, P < 0.01$; $F(4,40) = 3.19, P < 0.05$; $F(4,40) = 15.28, P < 0.0001$; $F(4,40) = 21.67, P < 0.0001$, respectively) (Figures 5e–h), but, this change was not significantly different between the AD-A and control LCLs. Instead, ALR, PLR, MRC were overall significantly higher in AD-A LCLs ($F(1,50) = 10.19, P < 0.0001$; $F(1,50) = 15.08, P < 0.0005$; $F(1,50) = 4.25, P < 0.05$, respectively).

Intracellular glutathione metabolism in LCLs

AD LCLs demonstrated lower GSH ($F(1,89) = 121.50, P < 0.001$) and GSH/GSSG ratio ($F(1,89) = 234.60, P < 0.0001$) and higher GSSG ($F(1,89) = 420.11, P < 0.0001$) as compared with control LCLs (see Supplementary Figure S2).

Compared with control LCLs, the two AD LCL subgroups demonstrated significantly lower GSH (AD-A: $F(1,53) = 200.18, P < 0.0001$; AD-N: $F(1,35) = 14.46, P < 0.001$) and GSH/GSSG (AD-A: $F(1,53) = 443.66, P < 0.0001$; AD-N: $F(1,35) = 92.89, P < 0.0001$) and significantly higher GSSG (AD-A: $F(1,53) = 114.19, P < 0.0001$; AD-N: $F(1,35) = 131.78, P < 0.0001$), however neither GSH, GSSG

nor GSH/GSSG ratio were significantly different between the two AD LCL subgroups (see Supplementary Figure S2).

Pretreatment with NAC increased intracellular GSH and the GSH/GSSG ratio and reduced GSSG in both the AD-A (GSH: $F(1,53) = 783.69$, $P < 0.0001$; GSSG: $F(1,53) = 810.73$, $P < 0.0001$; GSH/GSSG: $F(1,53) = 1264.48$, $P < 0.0001$) and AD-N (GSH: $F(1,35) = 87.34$, $P < 0.0001$; GSSG: $F(1,35) = 22.50$, $P < 0.0001$; GSH/GSSG: $F(1,35) = 110.22$, $P < 0.0001$) LCLs as compared with these LCLs before pretreatment (see Supplementary Figure S2).

DISCUSSION

This study examined the mitochondrial function in immune cells derived from children with AD at baseline and after exposure to an agent that increased ROS levels *in vitro*. Here, for the first time, we show that LCLs derived from children with AD exhibit significant abnormalities in mitochondrial respiration after exposure to increasing levels of ROS. Specifically, we demonstrate atypical simultaneous increases in ALR and PLR along with a sharp drop in RC when exposed to ROS in the AD LCLs as compared with the control LCLs. We then further demonstrate that these atypical responses were driven by a subset that comprised 44% of the AD LCLs. This subgroup also demonstrated an increase in MRC, further resulting in an increase in RC when the LCLs were not exposed to ROS. The atypical response to increased ROS in this AD LCL subgroup was prevented by an NAC pretreatment. Overall, this study demonstrates that at least a subset of LCLs derived from children with AD may have physiological abnormalities in mitochondrial function that are associated with abnormalities in oxidative stress. This evidence provides important insight into the potential pathophysiological mechanisms associated with AD and potential pathways for treatment.

Differences in RC depletion in AD LCL subgroups with ROS exposure

The adaptive response to ROS were divided into normal (AD-N) and abnormal (AD-A) subgroups. Exposure to ROS resulted in a more precipitous decrease in RC in the AD-A as compared with the AD-N LCLs. This is significant since reduced RC is linked to several diseases such as aging,³¹ heart disease³² and neurodegenerative disorders.^{33,34} In addition, when RC is depleted, apoptosis ensues resulting in reduced cell viability.³⁵ Differences in the dynamics between ALR and PLR in the AD LCL subgroups accounted for subgroup-specific responses.

In the AD-N subgroup, neither ALR nor PLR changed significantly, on average, as ROS increased. On an individual LCL level, we found a negative relationship between the change in ALR and PLR with increasing ROS. AD-N LCLs demonstrated an increase in ALR or PLR in response to increasing ROS, whereas the respiratory parameter that did not increase (ALR or PLR) decreased. This resulted in stable basal respiration as basal respiration is the combination of ALR and PLR. This, in turn, limited the decrease in RC as RC is the difference between MRC and basal respiration. These observations suggest that AD-N LCLs respond to increased ROS with one of two mechanisms: either increasing PLR or ALR, but not both.

For AD-A LCLs, the simultaneous increase in both ALR and PLR, on average and possibly on an individual level, resulted in a basal respiration increase which, when subtracted from MRC, results in a decrease in RC. Thus, this accounts for the greater decrease in RC in AD-A LCLs as compared with AD-N LCLs. This also suggests that ALR and PLR are required to work together to respond to increased ROS in the AD-A LCLs. Interestingly, the control LCLs demonstrated a significant positive relationship between ALR and PLR, yet did not demonstrate the same depletion in RC as the AD-A LCLs. This suggests that the AD-A are using the same mechanisms as the control LCLs to respond to the increases

ROS but cannot sustain this response properly, most likely because these ROS control mechanisms are inadequate in the context of chronic elevations in ROS. Alternatively, it appears that the AD-N LCLs have adapted to control for acute increases in ROS differently than control, probably as a consequence of chronic elevations in ROS.

RC depletion appears to be maximal at about 10 μM DMNQ. In fact ALR and PLR appear to peak at 10 μM DMNQ and then decrease at higher DMNQ concentrations. This decrease in ALR and PLR at high DMNQ concentrations most likely represents a failure of the mitochondria to function after RC is depleted. As depletion in RC results in reduced viability, it is likely that an apoptotic cascade is initiated when RC is depleted. This depletion most likely occurs faster as DMNQ concentration increases. As the LCLs are exposed to DMNQ for the same period of time regardless of the DMNQ concentration, it is likely that the LCLs exposed to DMNQ concentrations higher than 10 μM will have greater cellular damage after the 1h exposure and this will be reflected in the measurements of the respiratory parameters during the assay.

NAC rescues the atypical mitochondrial respiratory response in AD-A LCLs

Pretreatment of the AD-A LCL subgroup with NAC improved glutathione redox status and improved mitochondrial respiration. Interestingly, NAC did not normalize respiratory parameters but rather increased the ability of the cell to produce adenosine triphosphate (ATP) and maintain an adequate maximum respiratory capacity in the context of increased ROS. This suggests that an insufficient antioxidant capacity could contribute to the vulnerability of the mitochondrial to ROS and suggests that the AD-A LCL subset we have identified are particularly dependent on the cellular redox status. Interestingly, NAC may be efficacious in treating drug dependence,³⁶ schizophrenia,³⁷ bipolar depression,³⁸ trichotillomania³⁹ and may have a role in the treatment of Alzheimer's disease.^{40,41} Recent studies suggest that NAC has a role in supporting mitochondrial metabolism,³⁸ including mitigating oxidative stress-induced mitochondrial dysfunction,^{42,43} attenuating mitochondrial-related oxidative stress⁴⁴ and restoring cognitive deficits in a mouse model with complex I deficiency.⁴⁵ In a recent small double-blind placebo-controlled trial, NAC significantly improved irritability and social cognition in ASD children.⁴⁶

Molecular mechanisms associated with the increase in ATP-linked respiration

Elevations in ALR in the AD-A LCL subgroup is consistent with clinical reports of electron transport chain (ETC) overactivity in ASD children. Frye and Naviaux⁴⁷ reported five ASD/MD children with complex IV overactivity and Graf *et al*⁴⁸ reported a ASD/MD child with complex I overactivity. The fact that ALR increases in response to increased ROS, suggests that increased ATP production may be an important cytoprotective mechanism against ROS. MRC is a measure of the maximum ability of the ETC to generate ATP. Higher MRC in the AD-A subgroup is consistent with an overall increase in ALR and, again, suggests an overactivity of the ETC in the AD-A LCLs.

Molecular mechanisms associated with the increased PLR

Proton leak reduces the mitochondrial membrane potential which, in turn, decreases ETC ROS generation.⁴⁹ Proton leak is modulated by several mechanisms, including the adenine translocator and, in lymphocytes, uncoupling protein 2.⁵⁰ Given that uncoupling protein 2 is upregulated by chronic oxidative stress^{51,52} and that AD LCLs have chronic elevations in ROS,²⁰ it is possible that an increase in uncoupling protein 2 could be associated with the increase in PLR in the AD-A subgroup. However, as an increase in

mitochondrial membrane potential can increase both PLR and ALR,⁵³ an increase in mitochondrial membrane potential, potentially driven by ETC complex overactivity, could also account for the findings in the AD-A subgroup. Further research will be needed to clarify the molecular mechanisms leading to our findings.

MD and dysfunction in ASD

The nature and prevalence of MD in ASD is still under investigation. A recent meta-analysis found that 5% of children with ASD meet criteria for a classic MD but that 30+% of children in the general ASD population exhibit biomarkers consistent with MD.³ Recently, Frye⁵⁴ demonstrated that 50+% of ASD children have biomarkers of MD that are consistently abnormal (that is, repeatable) and valid (that is, correlate with other MD biomarkers). In another study, 80% of the children with ASD demonstrated abnormal lymphocytes ETC function.⁵⁵ Interestingly some children with ASD/MD have ETC overactivity rather than ETC deficiencies^{47,48} and many ASD/MD cases do not manifest lactate elevation,^{47,56,57} a key biomarker commonly used to identify individuals with classic MD. This has raised the idea that children with ASD might have a type of mitochondrial dysfunction that is more prevalent and distinct from classic MD. This study has demonstrated a new type of mitochondrial dysfunction that may be the result of redox abnormalities and could affect a significant number of children with ASD. In fact, the LCL subgroup with mitochondrial abnormalities represented 44% of the total AD LCLs examined.

Limitations

The number of subgroups that could be identified depended on the total number of LCLs examined, which was limited. Future studies will need to examine a larger number of LCLs to confirm these findings and determine whether there are multiple LCL subgroups. In addition, studies need to verify these findings in better matched control samples. Age-matched controls LCLs will be very useful as they become available and matching to typically developing sibling LCLs may be an extremely powerful method to relate the mitochondria metabolism phenotype uncovered in this study specifically to autism.

CONCLUSIONS

This study has identified a novel pattern of mitochondrial dysfunction in immune cells derived from AD children that appears to be present in a significant subgroup of LCLs. Thus, we demonstrate a new type of mitochondrial disorder that may affect a significant subgroup of AD children and provide insight into the interactions between systems that have been independently demonstrated to be abnormal in ASD.¹⁸ This information provides insight into the pathophysiology associated with ASD and a pathway for designing medical treatments for ASD.

CONFLICT OF INTEREST

The authors declare no conflict of interest.

ACKNOWLEDGMENTS

This research was funded by the National Institute for Child Health and Development (SJJ), the Arkansas Biosciences Institute (REF, SJJ), and the Jane Botsford Johnson Foundation (REF).

REFERENCES

1 American Psychiatric Association. *Diagnostic and Statistical Manual of Mental Disorders*, 4th edn. American Psychiatric Association: Washington, DC, USA, 1994.

- 2 Autism and Developmental Disabilities Monitoring Surveillance Year Principal Investigators, Centers for Disease Control and Prevention Prevalence of autism spectrum disorders—Autism and Developmental Disabilities Monitoring Network, United States, 2006. *MMWR Surveill Summ* 2009; **58**: 1–20.
- 3 Rossignol DA, Frye RE. Mitochondrial dysfunction in autism spectrum disorders: a systematic review and meta-analysis. *Mol Psychiatry* 2012; **17**: 290–314.
- 4 Fowler BA, Woods JS. Ultrastructural and biochemical changes in renal mitochondria during chronic oral methyl mercury exposure: the relationship to renal function. *Exp Mol Pathol* 1977; **27**: 403–412.
- 5 Shenker BJ, Guo TL, O I, Shapiro IM. Induction of apoptosis in human T-cells by methyl mercury: temporal relationship between mitochondrial dysfunction and loss of reductive reserve. *Toxicol Appl Pharmacol* 1999; **157**: 23–35.
- 6 Goyer RA. Toxic and essential metal interactions. *Annu Rev Nutr* 1997; **17**: 37–50.
- 7 Pourahmad J, Mihajlovic A, O'Brien PJ. Hepatocyte lysis induced by environmental metal toxins may involve apoptotic death signals initiated by mitochondrial injury. *Adv Exp Med Biol* 2001; **500**: 249–252.
- 8 Hiura TS, Li N, Kaplan R, Horwitz M, Seagrave JC, Nel AE. The role of a mitochondrial pathway in the induction of apoptosis by chemicals extracted from diesel exhaust particles. *J Immunol* 2000; **165**: 2703–2711.
- 9 Wong PW, Garcia EF, Pessah IN. ortho-substituted PCB95 alters intracellular calcium signaling and causes cellular acidification in PC12 cells by an immunophilin-dependent mechanism. *J Neurochem* 2001; **76**: 450–463.
- 10 Sherer TB, Richardson JR, Testa CM, Seo BB, Panov AV, Yagi T et al. Mechanism of toxicity of pesticides acting at complex I: relevance to environmental etiologies of Parkinson's disease. *J Neurochem* 2007; **100**: 1469–1479.
- 11 Yamano T, Morita S. Effects of pesticides on isolated rat hepatocytes, mitochondria, and microsomes II. *Arch Environ Contam Toxicol* 1995; **28**: 1–7.
- 12 Samavati L, Lee I, Mathes I, Lottspeich F, Huttemann M. Tumor necrosis factor alpha inhibits oxidative phosphorylation through tyrosine phosphorylation at subunit I of cytochrome c oxidase. *J Biol Chem* 2008; **283**: 21134–21144.
- 13 Vempati UD, Diaz F, Barrientos A, Narisawa S, Mian AM, Millan JL et al. Role of cytochrome C in apoptosis: increased sensitivity to tumor necrosis factor alpha is associated with respiratory defects but not with lack of cytochrome C release. *Mol Cell Biol* 2007; **27**: 1771–1783.
- 14 Suematsu N, Tsutsui H, Wen J, Kang D, Ikeuchi M, Ide T et al. Oxidative stress mediates tumor necrosis factor-alpha-induced mitochondrial DNA damage and dysfunction in cardiac myocytes. *Circulation* 2003; **107**: 1418–1423.
- 15 Vali S, Mythri RB, Jagatha B, Padiadpu J, Ramanujan KS, Andersen JK et al. Integrating glutathione metabolism and mitochondrial dysfunction with implications for Parkinson's disease: a dynamic model. *Neuroscience* 2007; **149**: 917–930.
- 16 Fernandez-Checa JC, Kaplowitz N, Garcia-Ruiz C, Colell A, Miranda M, Mari M et al. GSH transport in mitochondria: defense against TNF-induced oxidative stress and alcohol-induced defect. *Am J Physiol* 1997; **273**: G7–17.
- 17 Hallmayer J, Cleveland S, Torres A, Phillips J, Cohen B, Torigoe T et al. Genetic heritability and shared environmental factors among twin pairs with autism. *Arch Gen Psychiatry* 2011; **68**: 1095–1102.
- 18 Rossignol DA, Frye RE. A review of research trends in physiological abnormalities in autism spectrum disorders: immune dysregulation, inflammation, oxidative stress, mitochondrial dysfunction and environmental toxicant exposures. *Mol Psychiatry* 2012; **17**: 389–401.
- 19 James SJ, Melnyk S, Jernigan S, Cleves MA, Halsted CH, Wong DH et al. Metabolic endophenotype and related genotypes are associated with oxidative stress in children with autism. *Am J Med Genet B Neuropsychiatr Genet* 2006; **141B**: 947–956.
- 20 James SJ, Rose S, Melnyk S, Jernigan S, Blossom S, Pavliv O et al. Cellular and mitochondrial glutathione redox imbalance in lymphoblastoid cells derived from children with autism. *FASEB J* 2009; **23**: 2374–2383.
- 21 Melnyk S, Fuchs GJ, Schulz E, Lopez M, Kahler SG, Fussell JJ et al. Metabolic imbalance associated with methylation dysregulation and oxidative damage in children with autism. *J Autism Dev Disord* 2012; **42**: 367–377.
- 22 Rose S, Melnyk S, Pavliv O, Bai S, Nick TG, Frye RE et al. Evidence of oxidative damage and inflammation associated with low glutathione redox status in the autism brain. *Transl Psychiatry* 2012; **2**: e134.
- 23 Rose S, Melnyk S, Trusty TA, Pavliv O, Seidel L, Li J et al. Intracellular and extracellular redox status and free radical generation in primary immune cells from children with autism. *Autism Res Treat* 2012; **2012**: 986519.
- 24 Oh JH, Kim YJ, Moon S, Nam HY, Jeon JP, Lee JH et al. Genotype instability during long-term subculture of lymphoblastoid cell lines. *J Human Genet* 2013; **58**: 16–20.
- 25 Nickles D, Madireddy L, Yang S, Khankhanian P, Lincoln S, Hauser SL et al. In depth comparison of an individual's DNA and its lymphoblastoid cell line using whole genome sequencing. *BMC Genomics* 2012; **13**: 477.
- 26 Dranka BP, Hill BG, Darley-Usmar VM. Mitochondrial reserve capacity in endothelial cells: The impact of nitric oxide and reactive oxygen species. *Free Radic Biol Med* 2010; **48**: 905–914.

- 27 Melnyk S, Pogribna M, Pogribny I, Hine RJ, James SJ. A new HPLC method for the simultaneous determination of oxidized and reduced plasma amino thiols using coulometric electrochemical detection. *J Nutr Biochem* 1999; **10**: 490–497.
- 28 Laird NM, Ware JH. Random-effects models for longitudinal data. *Biometrics* 1982; **38**: 963–974.
- 29 Ward JH. Hierarchical grouping to optimize an objective function. *J Am Stat Soc* 1963; **77**: 841–847.
- 30 Anderberg M. *Cluster Analyses for Applications*. Academic Press: New York, NY, USA, 1973.
- 31 Desler C, Hansen TL, Frederiksen JB, Marcker ML, Singh KK, Juel Rasmussen L. Is there a link between mitochondrial reserve respiratory capacity and aging? *J Aging Res* 2012; **2012**: 192503.
- 32 Sansbury BE, Jones SP, Riggs DW, Darley-Usmar VM, Hill BG. Bioenergetic function in cardiovascular cells: the importance of the reserve capacity and its biological regulation. *Chem Biol Interact* 2011; **191**: 288–295.
- 33 Nicholls DG. Spare respiratory capacity, oxidative stress and excitotoxicity. *Biochem Soc Trans* 2009; **37**: 1385–1388.
- 34 Yadava N, Nicholls DG. Spare respiratory capacity rather than oxidative stress regulates glutamate excitotoxicity after partial respiratory inhibition of mitochondrial complex I with rotenone. *J Neurosci* 2007; **27**: 7310–7317.
- 35 Hill BG, Dranka BP, Zou L, Chatham JC, Darley-Usmar VM. Importance of the bioenergetic reserve capacity in response to cardiomyocyte stress induced by 4-hydroxynonenal. *Biochem J* 2009; **424**: 99–107.
- 36 Schmaal L, Berk L, Hulstijn KP, Cousijn J, Wiers RW, van den Brink W. Efficacy of N-acetylcysteine in the treatment of nicotine dependence: a double-blind placebo-controlled pilot study. *Eur Addict Res* 2011; **17**: 211–216.
- 37 Boulanger LM, Shatz CJ. Immune signalling in neural development, synaptic plasticity and disease. *Nat Rev Neurosci* 2004; **5**: 521–531.
- 38 Dean O, Giorlando F, Berk M. N-acetylcysteine in psychiatry: current therapeutic evidence and potential mechanisms of action. *J Psychiatry Neurosci* 2011; **36**: 78–86.
- 39 Grant JE, Odlaug BL, Kim SW. N-acetylcysteine, a glutamate modulator, in the treatment of trichotillomania: a double-blind, placebo-controlled study. *Arch Gen Psychiatry* 2009; **66**: 756–763.
- 40 Adair JC, Knoefel JE, Morgan N. Controlled trial of N-acetylcysteine for patients with probable Alzheimer's disease. *Neurology* 2001; **57**: 1515–1517.
- 41 Hsiao YH, Kuo JR, Chen SH, Gean PW. Amelioration of social isolation-triggered onset of early Alzheimer's disease-related cognitive deficit by N-acetylcysteine in a transgenic mouse model. *Neurobiol Dis* 2012; **45**: 1111–1120.
- 42 Gonzalez R, Ferrin G, Hidalgo AB, Ranchal I, Lopez-Cillero P, Santos-Gonzalez M et al. N-acetylcysteine, coenzyme Q10 and superoxide dismutase mimetic prevent mitochondrial cell dysfunction and cell death induced by d-galactosamine in primary culture of human hepatocytes. *Chem Biol Interact* 2009; **181**: 95–106.
- 43 Kuo HT, Lee JJ, Hsiao HH, Chen HW, Chen HC. N-acetylcysteine prevents mitochondria from oxidative injury induced by conventional peritoneal dialysate in human peritoneal mesothelial cells. *Am J Nephrol* 2009; **30**: 179–185.
- 44 Moreira PI, Harris PL, Zhu X, Santos MS, Oliveira CR, Smith MA et al. Lipoic acid and N-acetyl cysteine decrease mitochondrial-related oxidative stress in Alzheimer disease patient fibroblasts. *J Alzheimers Dis* 2007; **12**: 195–206.
- 45 Otte DM, Sommersberg B, Kudin A, Guerrero C, Albayram O, Filiou MD et al. N-acetyl cysteine treatment rescues cognitive deficits induced by mitochondrial dysfunction in G72/G30 transgenic mice. *Neuropsychopharmacology* 2011; **36**: 2233–2243.
- 46 Hardan AY, Fung LK, Libove RA, Obukhanych TV, Nair S, Herzenberg LA et al. A randomized controlled pilot trial of oral N-acetylcysteine in children with autism. *Biol Psychiatry* 2012; **71**: 956–961.
- 47 Frye RE, Naviaux RK. Autistic disorder with complex IV overactivity: a new mitochondrial syndrome. *J Pediatr Neurol* 2011; **9**: 427–434.
- 48 Graf WD, Marin-Garcia J, Gao HG, Pizzo S, Naviaux RK, Markusic D et al. Autism associated with the mitochondrial DNA G8363A transfer RNA(Lys) mutation. *J Child Neurol* 2000; **15**: 357–361.
- 49 Lambert AJ, Brand MD. Superoxide production by NADH:ubiquinone oxidoreductase (complex I) depends on the pH gradient across the mitochondrial inner membrane. *Biochem J* 2004; **382**: 511–517.
- 50 Azzu V, Jastroch M, Divakaruni AS, Brand MD. The regulation and turnover of mitochondrial uncoupling proteins. *Biochim Biophys Acta* 2010; **1797**: 785–791.
- 51 Li LX, Skorpen F, Egeberg K, Jorgensen IH, Grill V. Uncoupling protein-2 participates in cellular defense against oxidative stress in clonal beta-cells. *Biochem Biophys Res Commun* 2001; **282**: 273–277.
- 52 Giardina TM, Steer JH, Lo SZ, Joyce DA. Uncoupling protein-2 accumulates rapidly in the inner mitochondrial membrane during mitochondrial reactive oxygen stress in macrophages. *Biochim Biophys Acta* 2008; **1777**: 118–129.
- 53 Divakaruni AS, Brand MD. The regulation and physiology of mitochondrial proton leak. *Physiology* 2011; **26**: 192–205.
- 54 Frye RE. Biomarker of abnormal energy metabolism in children with autism spectrum disorder. *N Am J Med Sci* 2012; **5**: 141–147.
- 55 Giulivi C, Zhang YF, Omanska-Klusek A, Ross-Inta C, Wong S, Hertz-Picciotto I et al. Mitochondrial dysfunction in autism. *JAMA* 2010; **304**: 2389–2396.
- 56 Frye RE. Novel cytochrome b gene mutations causing mitochondrial disease in autism. *J Pediatr Neurol* 2012; **10**: 35–40.
- 57 Frye RE, Melnyk S, Macfabe DF. Unique acyl-carnitine profiles are potential biomarkers for acquired mitochondrial disease in autism spectrum disorder. *Transl Psychiatry* 2013; **3**: e220.



This work is licensed under a Creative Commons Attribution-NonCommercial-NoDerivs 3.0 Unported License. To view a copy of this license, visit <http://creativecommons.org/licenses/by-nc-nd/3.0/>

Supplementary Information accompanies the paper on the Translational Psychiatry website (<http://www.nature.com/tp>)